The standard centrifuge method accurately measures vulnerability curves of long-vesselled olive stems

Uwe G. Hacke[1], Martin D. Venturas[2], Evan D. MacKinnon[2], Anna L. Jacobsen[2], John S. Sperry[3] and R. Brandon Pratt[2]

[1]Department of Renewable Resources, University of Alberta, Edmonton, AB T6G 2E3, Canada; [2]Department of Biology, California State University, 9001 Stockdale Hwy, Bakersfield, CA 93311, USA; [3]Biology Department, University of Utah, 257S 1400E, Salt Lake City, UT 84112, USA

Author for correspondence:
Uwe G. Hacke
Tel: +1 780 492 8511
Email: uwe.hacke@ualberta.ca

Summary

- The standard centrifuge method has been frequently used to measure vulnerability to xylem cavitation. This method has recently been questioned. It was hypothesized that open vessels lead to exponential vulnerability curves, which were thought to be indicative of measurement artifact.

- We tested this hypothesis in stems of olive (*Olea europea*) because its long vessels were recently claimed to produce a centrifuge artifact. We evaluated three predictions that followed from the open vessel artifact hypothesis: shorter stems, with more open vessels, would be more vulnerable than longer stems; standard centrifuge-based curves would be more vulnerable than dehydration-based curves; and open vessels would cause an exponential shape of centrifuge-based curves.

- Experimental evidence did not support these predictions. Centrifuge curves did not vary when the proportion of open vessels was altered. Centrifuge and dehydration curves were similar. At highly negative xylem pressure, centrifuge-based curves slightly overestimated vulnerability compared to the dehydration curve. This divergence was eliminated by centrifuging each stem only once.

- The standard centrifuge method produced accurate curves of samples containing open vessels, supporting the validity of this technique and confirming its utility in understanding plant hydraulics. Seven recommendations for avoiding artefacts and standardizing vulnerability curve methodology are provided.

Introduction

Centrifugal force can be used to create known negative pressure in the xylem of woody vascular plants (Holbrook *et al.*, 1995; Pockman *et al.*, 1995). Early experiments in spinning stems revealed that xylem conduits remained water-filled to significant negative pressures and that cavitation occurred at species-specific pressures (Pockman *et al.*, 1995). This first technique was then modified and formalized in Alder *et al.* (1997) and this method became the standard centrifuge technique broadly employed in plant hydraulic research.

The centrifuge method, as outlined in Alder *et al.* (1997) has now been used for nearly 20 yr to advance our understanding of how water transport in plant xylem is affected by drought (Sperry & Hacke, 2002; Jacobsen *et al.*, 2007) and freeze/thaw stress (Davis *et al.*, 1999; Pittermann & Sperry, 2006). Centrifugal force methods have allowed us to link xylem physiology with structural xylem features (Hacke *et al.*, 2001, 2006; Jacobsen *et al.*, 2005; Cai & Tyree, 2010; Lens *et al.*, 2010), to characterize xylem trade-offs (Hacke & Sperry, 2001; Pratt *et al.*, 2007a), to screen cavitation resistance in poplar and willow clones (Cochard

et al., 2007; Arango-Velez *et al.*, 2011; Schreiber *et al.*, 2011), to link drought tolerance and life history traits (Pratt *et al.*, 2007b), and to study drought-induced mortality of woody plants (Choat *et al.*, 2012; Plaut *et al.*, 2012; Anderegg *et al.*, 2013; Paddock *et al.*, 2013).

According to the protocol originally described by Alder *et al.* (1997), hydraulic conductivity (K_h) of xylem segments is measured before and after spinning them in a centrifuge rotor to generate negative xylem pressure (Fig. 1). Cavitated conduits quickly fill with gas and are no longer able to conduct water, which results in a reduction in K_h. The Alder *et al.* (1997) rotor design and method (subsequently referred to as the 'standard centrifuge method') was more recently modified with the goal of allowing measurements of conductivity while stem segments were spinning (Cochard *et al.*, 2005; Li *et al.*, 2008). These newer 'flow-centrifugation' methods can use either the 'cavitron' rotor design (Cochard *et al.*, 2005), or a modification of the original Alder *et al.* (1997) design (Li *et al.*, 2008). The standard centrifuge method fundamentally differs from the cavitron method. Although water does not move through the stem segment during centrifugation when the standard centrifuge method is used,
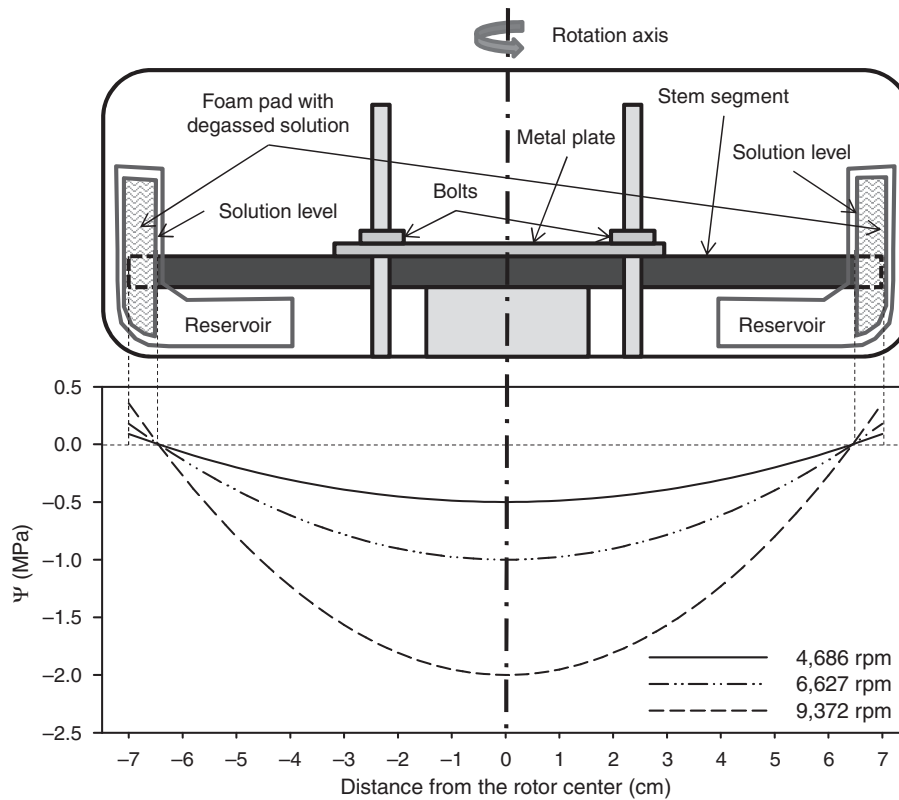
Fig. 1 Diagram showing sample placement in the standard centrifuge rotor and the pressure profile developed during spinning. The top sketch shows how the sample is set in the standard centrifuge rotor (Alder *et al.*, 1997). The stem segment is placed with its center crossing the rotation axis, and the ends are positioned within reservoirs containing degassed solution. Foam pads are placed in these reservoirs to avoid desiccation when the rotor is not spinning (Tobin *et al.*, 2013). The sample is secured in place with a metallic plate and bolts. The standard method requires the sample to be removed from the rotor after spinning it at a certain velocity for measuring its conductivity. Then it is mounted again for spinning it at a higher velocity (greater tension). Below the rotor sketch, the pressure (Ψ) profile developed within the conduits during spinning is represented for three different rotation velocities, calculated as determined by Alder *et al.* (1997). The minimum water potential (maximum stress) is reached in the center of the stem segment. At the intersections of the stem with reservoir solution the pressure is zero, and at the ends of the stem segment the pressure is positive. Note that with the standard centrifuge rotor, the pressure at both ends of the segment is equal while spinning, and therefore, there is no pressure-driven flow through the stem.

water movement during spinning is required for the cavitron method to estimate conductivity (Table 1).

When testing the cavitron, Cochard *et al.* (2010) found that the vulnerability curves of two species (*Quercus robur* and *Prunus persica*) differed depending on the size of the rotor that was used to generate the curves. When a smaller rotor was used (with stem segments 17.5 cm in length), curves tended to be more vulnerable than when a larger rotor was used (with segments 27.5 cm in length). For these two species with long vessels, both rotors produced exponentially shaped curves: that is, curves that showed an abrupt rise in cavitation at very modest xylem pressures. In two other species with shorter xylem conduits, better agreement between curves was found, regardless of rotor size and method used to generate the curves. An earlier study using the cavitron also showed inconsistent and nonreproducible curves for *Fraxinus excelsior*, another long-vesselled species (Cochard *et al.*, 2005; their fig. 2).

The mechanism behind the cavitron-specific artifact seems to be related to the flow of solution through segments during centrifugation (Wang *et al.*, 2014). The higher susceptibility to cavitation of short segments reported by Cochard *et al.* (2010) and the

extreme variability shown in Cochard *et al.* (2005) may be explained by the presence of impurities. Micro-bubbles and other particles may provide nucleating sites, which then grow when the pressure drops as the fluid moves toward the center of the segment, initiating cavitation during spinning (Sperry *et al.*, 2012; Rockwell *et al.*, 2014; Wang *et al.*, 2014). During centrifugation, pressures are not even throughout spinning segments with the minimum water potential (maximum xylem tension) occurring in the center of segments (Fig. 1). Hence, if vessels extend from one cut end to the center of the segment, nuclei would not be trapped by vessel ends and could trigger cavitation as they approached the center of the segment. In this way, cavitation would be triggered by introduced nuclei, rather than via air-seeding through vessel wall pores (for a discussion of the air-seeding mechanism, see Sperry & Hacke, 2004). The introduced nuclei artifact would at least partly explain why the cavitron has been affected by the open-vessel artifact whereas the standard centrifuge method does not appear to be susceptible to this artifact.

Although it is not clear how the standard centrifuge method could be prone to this potential artifact (because there is no flow through segments during spinning), artifacts are still possible if

Table 1 Characteristics of the main centrifuge techniques

Denomination	Improvements	Described in	Rotor	Stem segment length	Are stem segments ends immersed in reservoirs during spinning?	Hydraulic measures[a]
Original		Pockman et al. (1995)	Any	Variable (26–40 cm)	No, stem ends have to be trimmed before conductivity measurement	No flow
Standard		Alder et al. (1997)	Alder et al. (1997) design	Constant (usually 14 or 27 cm)	Yes	No flow
	Foam pads added to reservoir	Tobin et al. (2013)	Alder et al. (1997) design	Constant (usually 14 or 27 cm)	Yes, with foam pads	No flow
	Single-spin protocol	Present study	Alder et al. (1997) design	Constant (usually 14 or 27 cm)	Yes, with foam pads	No flow
Cavitron		Cochard et al. (2005)	Cochard et al. (2005) design	Constant (usually 17.5, 27.5 or 37.5 cm)	Yes	Flow
Flow centrifuge		Li et al. (2008)	Li et al. (2008) design	Constant (usually 27.5 cm)	Yes	Flow

[a]No flow, no induced flow during centrifugation; samples are removed from the rotor for performing conductivity measurements with the conductivity apparatus (Sperry et al., 1988) or the XY'LEM (Xylem Embolism Meter; Instrutec, Montigny les Cormeilles, France). Flow, stem segment conductivity is measured while spinning, and therefore, segments are only placed once in the rotor.

open vessels drain before the reservoir water reaches them when the centrifuge starts spinning (Choat et al., 2010). In addition, nucleating particles may be introduced into open vessels via perfusion with measuring solution before spinning in the centrifuge (Rockwell et al., 2014). The standard centrifuge protocol usually involves flushing of samples, although vacuum infiltration has also been used to remove embolism before generating a curve. Regardless of whether and how embolism is removed, conductivity is typically measured before centrifuging, and hence measuring solution is introduced into stem segments. Both the draining and the introduced nuclei ideas can be tested and protocols adjusted accordingly. For instance, if vessel draining were detected, it could be prevented in the future by using foam pads soaked with degassed solution as described by Tobin et al. (2013).

A recent report of erroneous curves produced by the standard centrifuge method is based on work with olive (Torres-Ruiz et al., 2014). According to this study, both the cavitron and the standard method overestimated vulnerability to cavitation relative to a dehydration method. The reported overestimations were higher as the sample length was shorter, suggesting that all centrifuge methods may be prone to the open vessel artifact. Based on such data, some have suggested that *all* exponential vulnerability curves would be incorrect, regardless of the method that was used to create the curves (Cochard & Delzon, 2013; Cochard et al., 2013). It has been argued that 'exponential curves are largely artifactual', and are likely based on 'faulty methods and data' (Cochard et al., 2013). Because many workers are coming to far-reaching conclusions in opinion papers and commentaries based on the accuracy or lack thereof of the standard centrifuge method (Rockwell et al., 2014), it is important to verify the reports that suggest that the standard method is prone to artifact.

Although scarcely mentioned in some commentaries (Cochard & Delzon, 2013), the standard method has been rigorously tested for short- and long-vesseled samples. Importantly, these studies

found no evidence for an open-vessel artifact when the Alder et al. (1997) rotor design was used, either with the standard method (segments removed from the rotor for conductivity measurements) or with the newer approach of measuring conductivity while the rotor is spinning (Li et al., 2008; Christman et al., 2012; Jacobsen & Pratt, 2012; Sperry et al., 2012; Tobin et al., 2013). The most recent example of such work examined dehydration and standard centrifuge curves measured on the same species at the same sites and during the same season (Jacobsen et al., 2014). Curves of 10 species were examined this way. In contrast to expectations based on the open vessel hypothesis, the use of these different methods did not result in a significant difference in xylem pressure causing 50% loss of conductivity (P_{50}), even though several of these species had long vessels (maximum vessel length > 1 m).

There is currently no consensus about the validity of the standard centrifuge method and other methods (Rockwell et al., 2014). Achieving such consensus is probably not a realistic expectation, nor is it required. However, additional data derived from clearly designed and carefully conducted experiments are likely necessary to move scientific discourse forward. If discrepancies are consistently found and are reproducible, then work may be directed toward identifying the cause of the discrepancies and toward improving the method. For instance, based on the work by Li et al. (2008) it seems reasonable to expect that the cavitron rotor design could be improved to eliminate or at least minimize artifacts.

Here we tested the standard centrifuge method by measuring vulnerability curves of current-year olive shoots, in part as a follow-up to the suggested measurement artifacts reported in Torres-Ruiz et al. (2014). A new variation of the standard centrifuge method was also tested. In this new 'single-spin' protocol, samples are centrifuged only once. The standard centrifuge method involves the removal of samples from the rotor after each spin. To test whether repeated mounting and
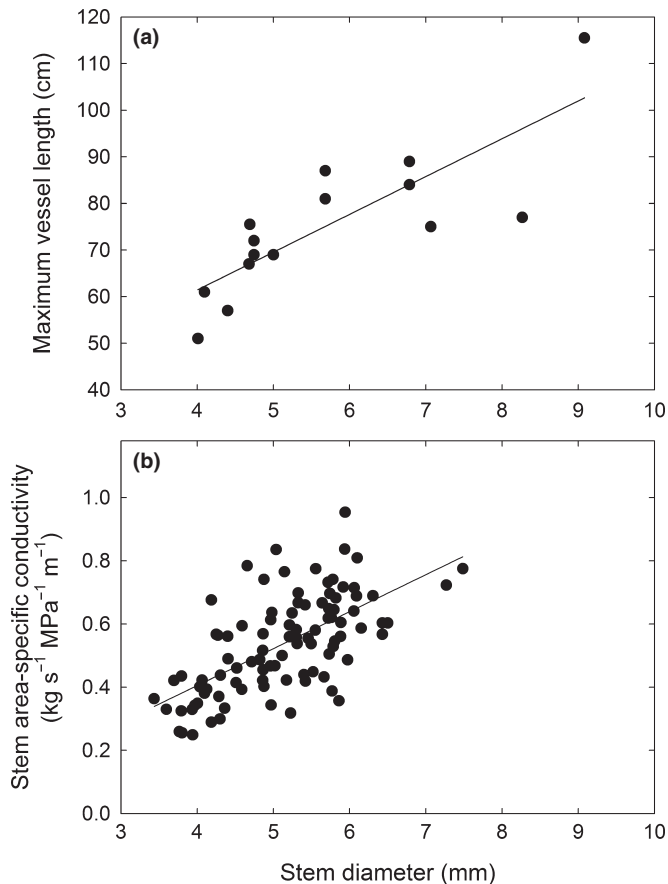
Fig. 2 (a) Maximum vessel length as a function of stem diameter measured in current-year growth of olive (*Olea europea*) trees ($r = 0.814$; $P < 0.001$). Maximum vessel length was determined by injecting air into the basal end of long branches. (b) Stem area-specific conductivity as a function of stem diameter ($r = 0.635$; $P < 0.001$).

removing of samples from the rotor causes reductions in conductivity, individual branch segments were exposed to a single xylem pressure as opposed to using the same segments at multiple pressures.

We used a hydraulic method for assessing vessel length (similar to that used by Torres-Ruiz *et al.*, 2014), tested for draining of open vessels, assessed whether there was a stem length effect, and compared centrifuge results to native stem conductivities. We took pains to eliminate as many sources of ambiguity as possible. We report stem area-specific conductivity (K_s) because recent studies have shown that percentage loss of conductivity (PLC) may be erroneously interpreted when K_s is not also evaluated in tandem (Jacobsen & Pratt, 2012; Sperry *et al.*, 2012). Furthermore, we measured K_s while accounting for passive uptake of water by stems; not doing so is an important source of error when dealing with low-conductivity material (Hacke *et al.*, 2000b; Torres-Ruiz *et al.*, 2012). We also assessed the impact of flushing on the shape of vulnerability curves. There is currently no agreement among researchers whether samples should be flushed before a vulnerability curve is constructed.

Three predictions of the open vessel artifact hypothesis were tested. (1) Shorter stems with a larger proportion of open vessels

would be more vulnerable than longer stems with a lower proportion of open vessels, as previously reported for olive (Torres-Ruiz *et al.*, 2014). (2) Centrifuge curves would be more vulnerable than dehydration curves. (3) The centrifuge-based vulnerability curve of a long-vesselled species, such as olive, would have an exponential shape due to introduced nuclei or draining of open vessels.

Materials and Methods

Plant material

Two sets of experiments were conducted for this study. The first set of measurements was conducted in September and October 2013. Long branches (1.5–2 m) were collected on 20 September 2013 from six irrigated olive (*Olea europea* L.) trees growing on or near the campus of California State University, Bakersfield, CA, USA, and from these stems *c.* 45-cm-long current year segments were cut underwater. The ends of stems were then wrapped in moist paper towels, and stems were placed in a large sealable plastic bag. The bag was kept at *c.* 4°C, and express-shipped to the University of Utah on the same day. Upon arrival at the University of Utah, samples were stored at *c.* 4°C. Centrifuge curves were measured on 24–27 September 2013. On 4 October 2013 at dawn, large branches between 1.43 and 1.90 m in length were cut from the same individuals described above and were used in Bakersfield for determination of native hydraulic conductivities and maximum vessel length. A second measurement campaign took place in January and February 2014. For this sampling, all stems were collected from one mature olive tree, which was also sampled in the first set of experiments. A single tree was used to reduce experimental variability for a set of targeted experiments. Because all measurements in 2014 were conducted in Bakersfield (between 22 January and 10 February 2014), samples were processed immediately after collection. All measurements were conducted on current year's shoots.

Maximum vessel length

In order to determine the maximum vessel length of current year's shoots, long branches were collected and injected with air from the proximal end at 100 kPa. During air injection, the distal part of stems was immersed in a water-filled tray. Stems were successively cut from their distal end, in 1-cm intervals, until the first bubbles appeared. To ensure that gas bubbles were travelling through xylem tissue, 1 cm of bark was removed from the distal end of stem segments following each cut so that only gas emerging from the cut xylem was observed. The end was then shaved underwater and fitted with a grommet and water-filled wide piece of plastic tubing so that the cut end could be carefully observed under ×10 magnification for emerging air bubbles. The longest vessel length was estimated as the length of the sample at the time that the first, single column of air bubbles was observed emerging from the xylem tissue. Fifteen lateral stems were used for maximum vessel length measures and injection-end stem diameters ranged from *c.* 4 to 9 mm.

Centrifuge vulnerability curves; flushing and vacuum infiltration treatments

Stem segments 3.5–7.5 mm in diameter were prepared by successively cutting them from longer stems underwater and trimming to the desired length with clippers and new razor blades. Hydraulic conductivity was measured with a conductivity apparatus as described previously (Sperry *et al.*, 2012). Conductivity was expressed per total stem cross-sectional area, calculated from mid-segment average stem diameter. A filtered (0.2 μm) 20 mM KCl measuring solution was made using purified water (distilled water passed through deionizing and organic removal cartridges; Barnstead E-Pure; Thermo Scientific, Waltham, MA, USA). Before and after each measurement of pressure-driven flow, background flow was measured. Dehydrated stem tissues can absorb water creating a negative background flow (water is driven off the balance) when there is no pressure head, and because olive stems had low conductivities, stable background flow measurements were important (Hacke *et al.*, 2000b). Hydraulic conductivity was calculated as the pressure-driven flow corrected for background flows divided by the pressure gradient. Maximum K_s was measured after stems were vacuum infiltrated (September 2013) or flushed at 100 kPa for 1 h (January 2014) with degassed and filtered (0.1 μm) 20 mM KCl solution. Solution was degassed using a membrane contactor (Liqui-Cel Minimodule 1.7 × 5.5, Charlotte, NC, USA).

We tested the effectiveness of flushing and vacuum infiltration treatments in removing embolism. A total of 18 stems were cut in air at 07:45h. Emboli were introduced on cutting. The stems were cut to a length of 14 cm and initial K_s values were measured. After that, nine stems were vacuum-infiltrated for 1 h with degassed 20 mM KCl solution at a vacuum pressure of −91 kPa. The remaining nine stem segments were flushed for 1 h with degassed and filtered 20 mM KCl solution at a pressure 100 kPa. Maximum K_s values were then measured. After that, the nine stems that initially flushed were vacuum-infiltrated and vice versa for the stems initially vacuum-infiltrated, again for 1 h. Conductivity was remeasured. Thus, if one procedure was more effective at removing emboli, it would be detected as a difference in K_s between paired stems exposed to the two methods.

Segments were spun in a custom-built rotor and vulnerability curves were generated as described previously (Alder *et al.*, 1997; Plavcova & Hacke, 2011; Tobin *et al.*, 2013). In September 2013, two different rotor diameters were used to test for an effect of segment length and fraction of open vessels. We measured vulnerability curves on 14- and 27-cm stem segments where the different stem lengths correspond to the different sizes of rotors. In January 2014, the smaller rotor design was used (14-cm segments). Vulnerability curves were constructed using both flushed stems and stems that were not flushed before the initiation of the curve. Curves were expressed by plotting PLC and/or K_s vs xylem pressure. Maximum K_s values measured in September and January/February were not statistically different ($P = 0.60$, *t*-test).

Samples were spun to nine xylem pressures. Moreover, we had to spin samples at very high rotational speed to induce high embolism levels. To test whether there was an effect associated with repeatedly handling and measuring the same segments, we constructed a 'single-spin' vulnerability curve. In this protocol, segments were spun only to a single xylem pressure. The single-spin centrifuge method required the use of more stems than the standard method. Although the standard curve was constructed with six to seven segments repeatedly spun at different xylem pressures, a total of 50 branches were used to construct the single-spin curve. For the single-spin approach, five to six stem segments were spun to each xylem pressure (Table 2).

Hydraulic detection of vessel length

We used an air-injection method for detecting the effect that embolized open vessels (vessels open to the segment center or beyond) have on hydraulic conductivity and PLC (see also Torres-Ruiz *et al.*, 2014). Current-year stem segments were vacuum infiltrated in 20 mM KCl solution for 1 h. Infiltrated stems were then injected at their proximal base with compressed nitrogen gas at 80 kPa for 10 min. This pressure is sufficient to allow spread of gas in vessels that are cut open, but is not high enough to force gas through vessel end walls (Sperry *et al.*, 2012). After injection, 3-cm-long stem segments at various distances from the injection site were cut from the stem underwater, and their K_s was measured before and after removing embolism by vacuum infiltration

Table 2 Centrifuge techniques used for evaluating *Olea europaea* cavitation vulnerability in Torres-Ruiz *et al.* (2014) and the present study

| Study | Centrifuge techniques | Measures per stem segment | Stem segment length (cm) | | No. stem segments | Flushed or vacuumed previous to spinning | Conductivity measurement | Background flow |
			Spun	Measured				
Torres-Ruiz *et al.* (2014)	Standard	Single	14 & 27	2–3 excised from the center[a]	3–7	Yes	Xyl'em or conductivity apparatus	Not reported
	Cavitron	Repeated	27.5	27.5	> 3	Yes	Meniscus	–
	Flow centrifuge	Repeated	14 & 27.5	14 & 27.5	> 3	Yes	Meniscus	–
Present study	Standard (foam pads improvement)	Repeated	14 & 27	14 & 27	6	Yes	Conductivity apparatus	Corrected for
	Standard (foam pads improvement)	Single	14	14	50	Yes	Conductivity apparatus	Corrected for

[a]This is not a standard procedure.

for 1 h. The first 3-cm segment was located 0 cm from the injected end (used as a control to verify that injection does indeed cause substantial embolism), the second segment was located at 7 cm from the injected end (7–10 cm from the end), and the third segment was located 13.5 cm from the injected end (13.5–16.5 cm from the end). These distances correspond with half of the segment length in the two rotors that differ in diameter. A K_s that is more depressed at 7 vs 13.5 cm indicates that more open vessels are present in the 14 vs 27 cm segments that were centrifuged. This approach of estimating vessel length is consistent with the method used in Torres-Ruiz *et al.* (2014) and provides a direct estimate of the hydraulic impact of open vessels in the center of a segment.

Native embolism and water potential measurements; air drying of branches

In order to measure native and benchtop-dehydrated conductivity, long stems (*c.* 2–3 m) were cut at predawn from the same trees used for constructing centrifuge curves. Small plastic bags were sealed onto four to five branchlets on each larger branch and then the larger branches were tightly triple-bagged in large plastic bags and rapidly transported to a laboratory. Branches were allowed to equilibrate for *c.* 2 h for native measures and 8–12 h for dehydrated branches. After equilibration, the bagged branchlets were collected and water potentials were measured using a pressure chamber (Model 2000; PMS Instrument Company, Albany, OR, USA). It was important to use multiple branchlets because even after many hours of equilibration there was still variability in water potential when stems were in a dehydrated state. The cut end of each branch was then held underwater and successive 10-cm cuts were made from the cut end, until the basal 1 m had been removed. Samples were then cut down further underwater, alternating cuts from the proximal and distal stem ends, until a central 14-cm-long segment was obtained. This gradual excision was done to relax xylem pressures before excising the final conductivity segment (Wheeler *et al.*, 2013). Hydraulic conductivity was then measured on these samples as described previously. PLC was calculated based on measurements of the maximum K_s as determined by vacuum infiltration or flushing.

Statistical analyses

Correlation analyses were used to test for an association between stem diameter and maximum vessel length and K_s. Vulnerability curves were analyzed via ANOVA (JMP v9.0; SAS Institute Inc., Carey, NC, USA). For curves generated by repeatedly spinning the same stems, the independent variables in the model included xylem pressure as a fixed factor and stem as a random factor. For curves generated by spinning different stems at each pressure, the model included xylem pressure as a fixed factor. The standard error from these different ANOVA models was used to generate 95% confidence intervals to compare conductivity between stems at a given xylem pressure that were either repeatedly spun in a centrifuge vs those spun only once at a given pressure. For comparing dehydration and single-spin VCs, PLC datasets were fitted to Weibull curves by least square means (LSM), and their P_{50} obtained from the curves. Bootstrapping was performed for propagating the uncertainty in these fits. The datasets were randomly resampled with replacement 1000 times to generate subsamples equal in size to the original datasets. Each subsample was fitted to a Weibull curve by LSM. P_{50} and the PLC at different pressures were obtained for each one of these curves, and the percentiles 2.5 and 97.5 were used to determine the 95% confidence intervals (CIs).

Results

Testing for the presence of open vessels

Maximum vessel length of current-year stems was 75.3 ± 4.0 cm ($\pm$ SE, $n = 15$) with a maximum of 116 cm (Fig. 2a). Maximum
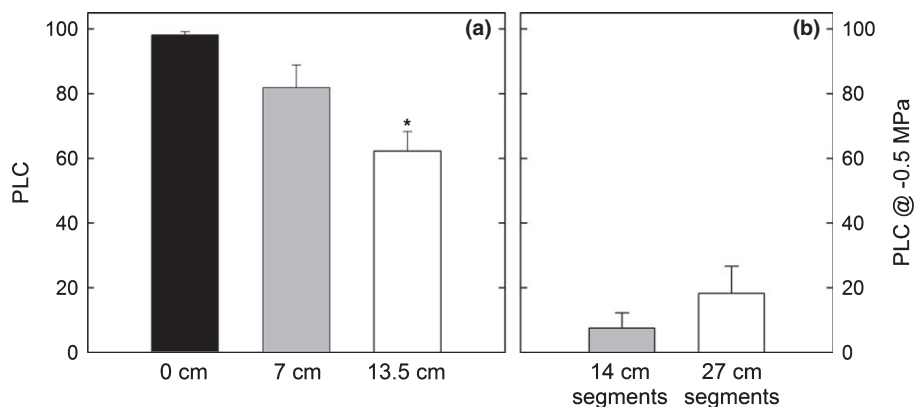
Fig. 3 (a) Percentage loss of hydraulic conductivity (PLC) of 3-cm-long segments located at different distances from the olive (*Olea europea*) stem ends that were injected with compressed nitrogen gas at mild pressure (80 kPa) (mean + 1 SE). Segments located 13.5 cm away from the injected end (white bar) had lower PLC (and fewer open vessels) than segments located 7 cm (gray bar) and 0 cm (black bar) away from the injected end ($P < 0.05$). (b) PLC of segments 14 and 27 cm in length after spinning to −0.5 MPa. If open vessels drained when the centrifuge rotor started spinning, then they should show similar PLC values as shown in (a). The asterisk in (a) indicates that the PLC of segments located 13.5 cm away from the injected end were significantly lower than the PLC of segments located 7 cm away from the injected end ($P = 0.030$).

vessel length was correlated with stem diameter; bigger stems tended to have longer vessels ($r = 0.814$; $P < 0.001$). K_s also increased with stem diameter (Fig. 2b) ($r = 0.635$; $P < 0.001$).

Injecting compressed nitrogen into stems led to nearly 100% loss in conductivity (PLC) directly at the cut end of the stem, as expected (PLC $= 98.2 \pm 1.0$, $n = 5$) (Fig. 3a). Short segments located 7 cm from the injected end had 81.8 ± 7.0 PLC, whereas segments located 13.5 cm from the injected end showed significantly less PLC (62.3 ± 6.0; $P = 0.030$, paired t-test, $n = 9$). These results indicated that the centrifuged shorter 14-cm stems had significantly more open vessels than the longer 27-cm stems. To test if open vessels drained when the centrifuge rotor began spinning, we plotted the PLC measured at -0.5 MPa for 14- and 27-cm-long segments (Fig. 3b). Draining of open vessels (open to center) should result in high PLC even at modest xylem tension and higher PLC in spun 14-cm segments. There was no evidence of vessel draining; PLC at -0.5 MPa was much lower than

the air-injected PLC values (Fig. 3a) and long segments were not significantly different in PLC than short ones.

Testing for an effect of segment length on centrifuge curves

Olive branches measured in September 2013 showed a gradual increase in PLC with decreasing xylem pressure, regardless of segment length (Fig. 4). These data were collected by using the standard method; that is, the same branch segments were exposed to increasingly negative xylem pressures. The P_{50} was -1.8 ± 0.3 and -2.1 ± 0.2 MPa for 27- and 14-cm segments, respectively (mean $\pm$ SE) (Fig. 4a). These P_{50} values were not significantly different ($P = 0.26$, t-test). When vulnerability curves were plotted as stem area-specific conductivity, the two curves were nearly identical (Fig. 4b).

Native values of stem area-specific conductivity and xylem pressure are shown in Fig. 4(b) (red triangles). These native values refer to branches collected at dawn during the same time that the samples for the centrifuge curves were collected and measured, and they closely matched the centrifuge-based vulnerability curves.

Testing for an effect of repeated spins on centrifuge curves

Standard and single-spin methods produced P_{50} values of -2.92 and -3.34 MPa, respectively (Fig. 5). Curves showed reasonable agreement and 95% confidence intervals of the means overlapped over much of the pressure range tested; however, curves diverged
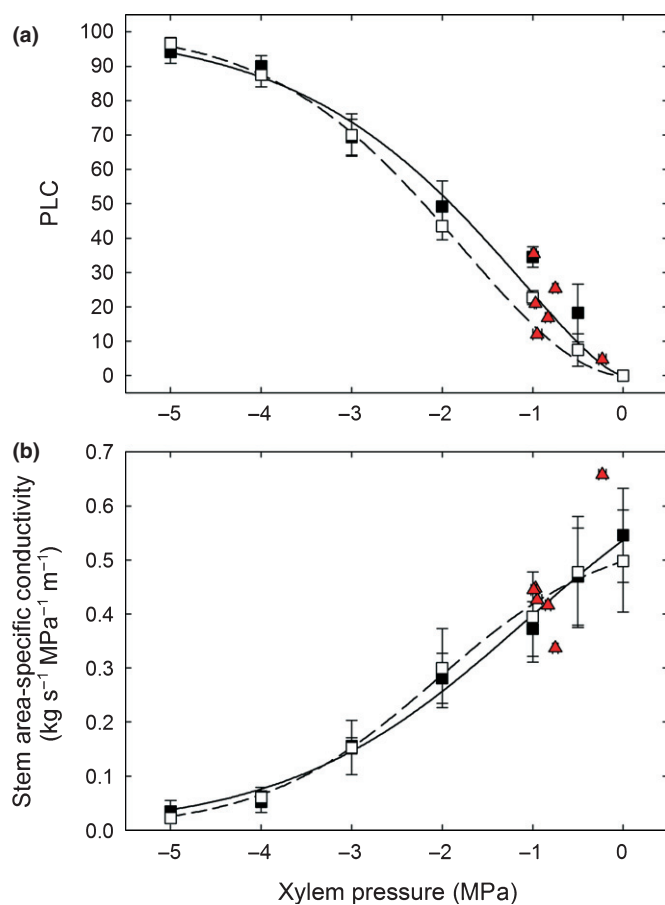
Fig. 4 (a) Effect of stem length on centrifuge vulnerability curves. Curves were measured in September 2013. Mean $\pm$ 1SE for 27-cm-long (closed squares, $n = 7$) and 14-cm-long segments (open squares, $n = 6$) of current-year extension growth. Native values of xylem pressure and stem area-specific conductivity (samples collected at predawn) are shown as red triangles for current-year growth. Each triangle represents one olive (*Olea europea*) tree; these same six trees were sampled for the vulnerability curves. A Weibull function was used to fit the percent loss of hydraulic conductivity (PLC) data. (b) Stem area-specific conductivity as a function of xylem pressure.
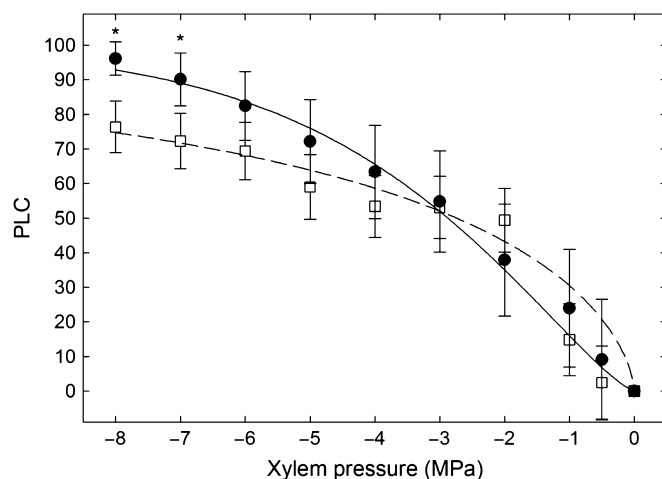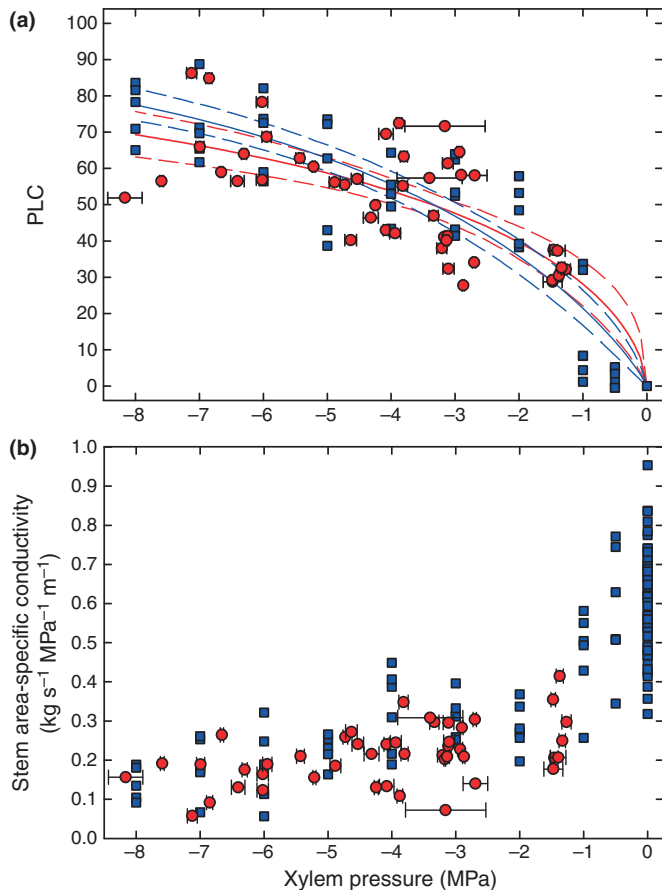

Fig. 5 Vulnerability curves showing percentage loss of hydraulic conductivity (PLC) as a function of xylem pressure. Means and 95% confidence intervals (CIs) are shown. Black circles and solid line, data obtained from using the standard centrifuge method, which involved repeated spins of the same stem segments ($n = 6$); open squares and dashed line, the 'single-spin method' ($n = 5$–6 per pressure). The single-spin protocol involves spinning segments to a single xylem pressure to avoid any fatigue that may be caused by repeated spins. CIs overlapped at all xylem pressures, except at the two most negative xylem pressures that were measured (indicated by asterisks). A Weibull function was used to fit the PLC data. All stems were collected from one mature olive (*Olea europea*) tree in January 2014.

at the most negative xylem pressures, indicating that repeated centrifuging of the same samples may cause overestimation of PLC. Both of the curves shown in Fig. 5 were slightly more resistant than the curve constructed in the previous fall, although the difference in P_{50} was not significant ($P = 0.10$, t-test using repeated spin data).

Comparison of centrifuge and dehydration curves

Data points derived from native conductivity measurements and dehydrated branches were in excellent agreement with the single-spin centrifuge curve (Fig. 6). Both methods had nearly identical P_{50} and curve shapes. The P_{50} (95% CI) of the dehydration and single-spin centrifuge curves were -3.36 (-3.91, -2.85) MPa and -3.33 (-3.79, -2.92) MPa, respectively. These are not statistically different because both confidence intervals overlap.

For the dehydration curve, in most cases, water potential measurements from individual branchlets of the same large branch produced similar values. In a few instances there was poor water potential equilibration despite the fact that branches were allowed to equilibrate for several hours. This occurred at c. -8 MPa, but there were also two instances in the pressure range between -3 and -4 MPa (see horizontal error bars in Fig. 6). Instead of discarding these data, we included them in our analysis and documented it. Removing the three data points exhibiting the greatest variation in water potentials shifted the P_{50} of the dehydration curve to be slightly more negative (-3.44 MPa), but this was still not significantly different from the P_{50} of the single-spin centrifuge curve (i.e. this value still falls within the 95% CI of the P_{50} of the single-spin centrifuge curve).

Comparison of flushed vs nonflushed samples and comparison of flushing vs vacuum infiltration treatments

Vulnerability curve shape differed depending on whether samples had been flushed before measurements to remove native embolism. Flushed segments had higher conductivities at xylem pressures > -2 MPa compared to samples that were not flushed (Fig. 7, asterisks). Further, conductivity of flushed samples decreased between 0 and -2 MPa indicating that olive stems had a population of vessels that cavitate at modest xylem tension. By contrast, at these same pressures the conductivity remained nearly constant in samples that were not flushed. As a result, these latter samples exhibited a sigmoidal curve shape. At xylem pressures of ≤ -2 MPa, curves converged. The approximate xylem pressure of stems at the time of collection was -2.5 MPa (vertical arrow in Fig. 7).

Both flushing and vacuum infiltration resulted in significant increases in K_s relative to initial measurements of K_s on
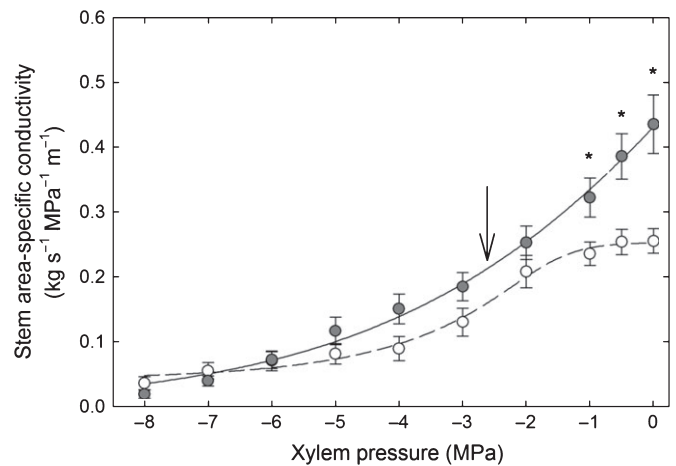

Fig. 6 Vulnerability curves showing (a) percentage loss of hydraulic conductivity (PLC) or (b) stem area-specific conductivity (K_s) as a function of xylem pressure using the single-spin centrifuge method (blue squares). Symbols represent individual olive (*Olea europea*) stem segments to show variability. Red circles show native PLC (a) and K_s (b) as a function of the xylem pressure branches experienced at the time of collection or after benchtop dehydration. Each circle represents one branch. Horizontal error bars show variation in xylem pressure for individual branches (means $\pm$ 1 SE, $n = 4$). A Weibull function was used to fit the PLC data in (a); solid blue line for single spin method and solid red line for dehydration and native PLC data, the dashed lines in the corresponding colors represent their 95% CIs.

Fig. 7 Stem area-specific conductivity (K_s) of olive (*Olea europea*) stem segments as a function of xylem pressure. Dark gray circles and solid line, segments that were flushed before centrifugation; open circles and dashed line, segments that were not flushed (means $\pm$ 1SE, $n = 6$). Vertical arrow shows the approximate xylem pressure of nonflushed samples at the time of collection. Asterisks indicate significant differences in K_s at individual xylem pressures ($P < 0.05$, t-test). Curves converged at xylem pressures ≤ -2 MPa.
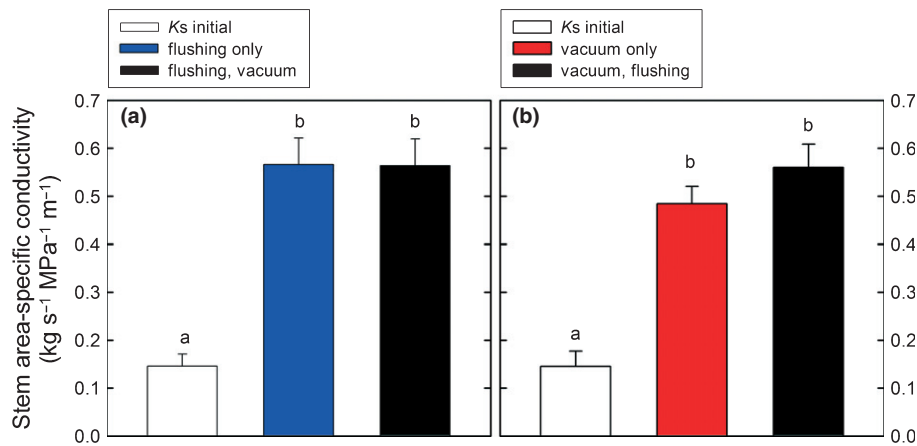
Fig. 8 Effectiveness of flushing and vacuum infiltration treatments to remove embolism in xylem. A total of 18 olive (*Olea europea*) stems were collected; stems were cut in air. (a) Nine stem segments were prepared and the initial stem area-specific conductivity (K_s) was determined (white bar). Segments were then flushed for 1 h to remove embolism (blue bar). Subsequently, segments were vacuum infiltrated for 1 h to test if K_s would increase further (black bar). (b) A second set of nine stem segments was vacuum infiltrated (red bar) and subsequently flushed (black bar). Although not significant at $P < 0.05$, flushing did cause a slight increase in K_s relative to vacuum infiltration. Unique letters indicate significant differences at $P < 0.05$ based on a one-way ANOVA. Values are means + SE.

embolized segments (Fig. 8) and flushing and vacuum infiltration were not different in their effectiveness at removing emboli.

Discussion

No effect of stem length on vulnerability curves

The data indicate that there was a higher fraction of open-to-center vessels in short (14 cm) compared to long (27 cm) centrifuged stems and that they would be expected to vary in their vulnerability to cavitation curves based on the hypothesized open vessel artifact. However, we found no difference in the vulnerability curves of stem samples of differing lengths and differing percentages of open vessels. If the standard centrifuge method was susceptible to the open vessel artifact hypothesis, we should have found that shorter segments were more vulnerable to cavitation than longer segments. Furthermore, if all open vessels became gas-filled due to draining, vulnerability curves should have shown an immediate rise to > 60 PLC based on the gas-injection data. Instead, curves did not exceed 60 PLC until pressures dropped below −2 MPa. These results agree with recent papers that found no stem-length effect in long-vesselled species such as *Vitis vinifera*, *Quercus wislizenii*, *Quercus robur*, *Prunus persica*, *Sorbus scopulina* and *Quercus gambelii*, when the standard centrifuge method was used (Jacobsen & Pratt, 2012; Sperry *et al.*, 2012; Tobin *et al.*, 2013). However, our findings are in striking contrast with cavitron data for *Prunus persica*, *Quercus robur*, *Fraxinus excelsior* and *Robinia pseudoacacia* (Cochard *et al.*, 2005, 2010; Wang *et al.*, 2014) indicating that these two different centrifuge methods do not produce similar results for long-vesselled species.

This raises the question of why different centrifuge methods provide different results. The explanation that is most consistent with the available data is that the cavitron is prone to the introduced nuclei artifact as solution flows through a segment during spinning (Wang *et al.*, 2014). As outlined in the Introduction, solution does not flow through segments in the standard method

(Table 1). In addition, the cavitron may have other design features that make it prone to introduced nuclei, because the flow method of Li *et al.* (2008) is apparently not prone to this same artifact.

Without the introduction of nuclei or draining of water from open vessels during initial rotor acceleration (before the stem ends become immersed in reservoir water), there is no obvious reason why open-to-center vessels should alter the process of cavitation. The water at the ends of the stem remain at (or above) atmospheric pressure during centrifugation (Fig. 1). Cavitation should occur in the middle of the stem where the pressures are most negative and where the vessel network (and air-seeding sites) remain intact and undisturbed.

Comparing centrifuge curves with native conductivities and data obtained from air drying

Dehydration curves are often considered as a benchmark for other methods. In the present study, we found good agreement between centrifuge-based data and dehydration-based data. Based on this result and the many recent studies that have found the same agreement between methods (Jacobsen *et al.*, 2007, 2014; Li *et al.*, 2008; Jacobsen & Pratt, 2012; Sperry *et al.*, 2012; Tobin *et al.*, 2013), we conclude that the standard centrifuge method can accurately measure vulnerability curves for long-vesselled species like olive. The accuracy of measurements can be maximized if samples are spun to a single pressure, but this protocol is more time-consuming and requires using many different stems, which may introduce additional experimental variability.

In contrast to our findings, Torres-Ruiz *et al.* (2014) reported P50 values of −0.9 and −2.8 MPa with their small (15 cm) and large (28 cm) rotor, respectively, when using the standard centrifuge method. However, a potentially important source of error relates to the fact that background flow was not consistently accounted for in the Torres-Ruiz *et al.* (2014) study (Table 2). We found that background flow had a large effect on K_s

measurements in olive. In addition, Torres-Ruiz *et al.* (2014) reported that their K_s values were highly variable and the actual K_s values for their vulnerability curve material were not reported. The wide variability they observed suggests that they were analyzing samples that were not directly comparable. Aside from an uneven and minimal ($n = 3$–7) sample size, their study is potentially confounded by seasonal effects because their short segment curves were all constructed in July, whereas their long segment curves were all measured in September. Moreover, their imaging data were collected in February and 3 yr after other measures. All of these factors make it difficult to interpret the Torres-Ruiz *et al.* (2014) findings and to deduce why their curves could not be reproduced.

Data supporting concerns about the accuracy of the standard centrifuge method also comes from work on grapevine (Choat *et al.*, 2010), a species with wide and relatively long vessels. The authors assumed that dehydration curves can be used as a reference for the centrifuge method. However, a follow-up study with long (> 3 m) grapevine shoots revealed that dehydration can lead to errors in determination of maximum K_s with time, and that this made it impossible to accurately use the relative measure of PLC for constructing vulnerability curves in this species (Jacobsen & Pratt, 2012). Gel formation is well described for *Vitis vinifera* cv Chardonnay, the variety Choat *et al.* (2010) examined, especially in response to embolism, wounding and infection (Sun *et al.*, 2008, 2013). McElrone *et al.* (2012) argued that Choat *et al.* (2010) avoided issues with tyloses/gel formation by dehydrating long stems and sampling at the center of these stems. However, despite the implication by McElrone *et al.* (2012), Jacobsen & Pratt (2012) sampled in much the same way as Choat *et al.* (2010) and their work revealed that gels formed at > 1 m from cut ends of long branches. Importantly, the Choat *et al.* (2010) study did not report area-specific conductivity in absolute units, relying instead on changes in PLC relative to a maximum (and presumably constant and reproducible) reference. As explained, the maximum K_s is prone to drift in grapevine. Absolute units are arguably preferable for fully interpreting vulnerability curves, especially if these curves are used to come to broad conclusions about the validity of methods. When gel formation was accounted for, dehydration and centrifuge curves in grapevine agreed (Jacobsen & Pratt, 2012).

Suggestions for future work

In vivo imaging has received interest as a new tool to assess vulnerability to cavitation. We caution that imaging (regardless of whether it involves dye perfusions, cryo-SEM, *in vivo* imaging or some other method) needs to be validated and paralleled by hydraulic measurements. Imaging techniques are not immune to artifacts (Canny, 1997; Cochard *et al.*, 2000; Pérez-Donoso *et al.*, 2007). In grapevine, it was found that gel-filled conduits could not be differentiated from water- or saline solution-filled conduits when examined using MRI (Pérez-Donoso *et al.*, 2007), suggesting that these images are of limited utility in estimating vessel hydraulic functionality. Hence, the need for using and, as necessary, improving hydraulic methods will remain. In the

interest of achieving consistency and accuracy in future plant hydraulic studies, we suggest the following practices which may have been important for avoiding artifacts in our study as well as others that have also shown no open vessel artifact.

(**1**) The Alder *et al.* (1997) rotor design is preferable to the cavitron rotor design, especially when long-vesselled species are studied. A potential source of error may occur by draining of cut vessels when the rotor is stopped or moving very slowly and stem ends are exposed to air (rather than being immersed in reservoir water). This error can easily be addressed by using foam pads in rotor reservoirs as described in Tobin *et al.* (2013), so that samples do not dry out between spins.

(**2**) Vulnerability curves should be reported with K_s in addition to PLC values. This is particularly evident for nonflushed samples. In many cases it is more informative to focus on the actual area-specific conductivities than on the PLC values (Jacobsen & Pratt, 2012; Sperry *et al.*, 2012), which are subject to drift or error in the maximum conductivity reference value. Even in the absence of reference drift, PLC is not the best basis for comparison because plants at 90 vs 10 PLC can actually have identical K_s and conducting capacities (Li *et al.*, 2008; Taneda & Sperry, 2008). Pratt *et al.* (2008) showed that when curves were reported with K_s values, stems and roots were not different in conductivity at the seasonal minimum predawn water potential. In other words, the long held view that roots tend to be more vulnerable to embolism may also be tied to the PLC vs K_s issue in some cases.

(**3**) It is arguably preferable to flush (or vacuum-infiltrate) samples before the construction of vulnerability curves. Flushing makes centrifuge curves comparable to dehydration data or native embolism measurements, because these latter measurements typically depend on measuring the maximum (flushed) conductivity. Curves reporting the PLC of nonflushed segments use native conductivity as their maximum reference, but native conductivity will vary with stem age, season, site and other factors. Such curves can only capture the vulnerability of xylem that is still functional under field conditions, and this may only be a small fraction, especially if the xylem is already highly embolized at the time of sampling. Because the curve only reflects more resistant xylem, one may erroneously conclude that there are no vulnerable vessels present and that there is a substantial margin of safety from cavitation. The potential discrepancy between flushed and nonflushed samples is particularly evident when curves are expressed as PLC (Sperry *et al.*, 2012; see their Fig. 5b).

As expected, the K_s of flushed and unflushed curves converge at the minimum xylem pressure that stems were exposed to in the field (Fig. 7). Hence, a flushed curve can readily be scaled to a nonflushed one for any desired xylem pressure (Pockman & Sperry, 2000). An unflushed curve, however, cannot predict the vulnerability of any cavitated xylem, and in this sense the unflushed curve contains less information.

Many reported curve shape discrepancies and the discussion of 'unrealistic' P_{50} values in the range between 0 and -0.5 MPa (Cochard *et al.*, 2013) may be tied to simple confusion over flushed vs unflushed curves. Nonflushed curves are *a priori* more likely to result in a sigmoid shape and more negative P_{50} values (Fig. 7), because they do not include the necessarily more

vulnerable vessels that were already cavitated before the curve was started. Meaningful comparisons of curve statistics require consistent scaling of flushed curves, typically to a characteristic field pressure of the species (Choat *et al.*, 2012).

(**4**) In dehydrated samples and samples with low conductivity (such as olive stems), it is crucial to determine the solution flow in the absence of an applied pressure gradient (Hacke *et al.*, 2000b). Water uptake by samples may be driven by osmotic and capillary uptake. Methods in which this 'background flow' is not determined can lead to significant errors that can affect accurate estimation of vulnerability to cavitation.

(**5**) Dehydration curves and native conductivities must be measured carefully. The relaxation of samples may be necessary to avoid cutting artifacts described as occurring for some species (Sperry, 2013; Wheeler *et al.*, 2013); however, it is also important to avoid hydrating for too long in some species as they can refill emboli before excision (Trifilo *et al.*, 2014). Estimates of native stem xylem pressure must also be made with caution on equilibrated tissue. When the xylem is highly embolized the pressure chamber values can become unreliable and other methods may be required (Tobin *et al.*, 2013). Using stem psychrometers in tandem with the pressure chamber can be used to diagnose such cases.

(**6**) Comparisons between techniques must not be confounded by inherent differences between individual plants, age, diameter, aspect, vigor and health of segments, time of year, sampling population, cavitation fatigue and sampling year. All of these sources of variation are potentially significant and should be controlled (Matzner *et al.*, 2001; Jacobsen *et al.*, 2007; Taneda & Sperry, 2008; Anderegg *et al.*, 2013).

(**7**) Curves for long-vessrelled species should be checked, for example by comparing stems of different length, or by comparison to native embolism or dehydration data. If the native and centrifuge data agree, those data should be regarded as valid regardless of the P_{50} or curve shape observed.

Conclusion

We showed that the standard centrifuge method accurately measured vulnerability curves in stems with open vessels. The presence of long vessels was not associated with having vulnerable xylem, suggesting that curve shape is not determined by the presence of open vessels. Many species exhibit an exponential loss in hydraulic conductivity, including roots of conifers where tracheids render them immune to any possibility of an open vessel artifact (Hacke *et al.*, 2000a; Pittermann *et al.*, 2006). A concerted attempt to standardize techniques and protocols across the field to those that have been repeatedly shown to be robust to artifact, such as those described in the present study, may help in achieving more accurate results.

Acknowledgements

References

Alder NN, Pockman WT, Sperry JS, Nuismer S. 1997. Use of centrifugal force in the study of xylem cavitation. *Journal of Experimental Botany* **48**: 665–674.

Anderegg WRL, Plavcová L, Anderegg LDL, Hacke UG, Berry JA, Field CB. 2013. Drought's legacy: multi-year hydraulic deterioration underlies widespread aspen forest die-off and portends increased future risk. *Global Change Biology* **19**: 1188–1196.

Arango-Velez A, Zwiazek JJ, Thomas BR, Tyree MT. 2011. Stomatal factors and vulnerability of stem xylem to cavitation in poplars. *Physiologia Plantarum* **143**: 154–165.

Cai J, Tyree MT. 2010. The impact of vessel size on vulnerability curves: data and models for within-species variability in saplings of aspen, *Populus tremuloides* Michx. *Plant, Cell & Environment* **33**: 1059–1069.

Canny MJ. 1997. Vessel contents during transpiration: embolisms and refilling. *American Journal of Botany* **84**: 1223–1230.

Choat B, Drayton WM, Brodersen C, Matthews MA, Shackel KA, Wada H, Mcelrone AJ. 2010. Measurement of vulnerability to water stress-induced cavitation in grapevine: a comparison of four techniques applied to a long-vess\-eled species. *Plant, Cell & Environment* **33**: 1502–1512.

Choat B, Jansen S, Brodribb TJ, Cochard H, Delzon S, Bhaskar R, Bucci SJ, Feild TS, Gleason SM, Hacke UG et al. 2012. Global convergence in the vulnerability of forests to drought. *Nature* **491**: 752–755.

Christman MA, Sperry JS, Smith DD. 2012. Rare pits, large vessels and extreme vulnerability to cavitation in a ring-porous tree species. *New Phytologist* **193**: 713–720.

Cochard H, Badel E, Herbette S, Delzon S, Choat B, Jansen S. 2013. Methods for measuring plant vulnerability to cavitation: a critical review. *Journal of Experimental Botany* **64**: 4779–4791.

Cochard H, Bodet C, Ameglio T, Cruiziat P. 2000. Cryo-scanning electron microscopy observations of vessel content during transpiration in walnut petioles. Facts or artifacts? *Plant Physiology* **124**: 1191–1202.

Cochard H, Casella E, Mencuccini M. 2007. Xylem vulnerability to cavitation varies among poplar and willow clones and correlates with yield. *Tree Physiology* **27**: 1761–1767.

Cochard H, Damour G, Bodet C, Tharwat I, Poirier M, Améglio T. 2005. Evaluation of a new centrifuge technique for rapid generation of xylem vulnerability curves. *Physiologia Plantarum* **124**: 410–418.

Cochard H, Delzon S. 2013. Hydraulic failure and repair are not routine in trees. *Annals of Forest Science* **70**: 659–661.

Cochard H, Herbette S, Barigah T, Badel E, Ennajeh M, Vilagrosa A. 2010. Does sample length influence the shape of xylem embolism vulnerability curves? A test with the Cavitron spinning technique. *Plant, Cell & Environment* **33**: 1543–1552.

Davis SD, Sperry JS, Hacke UG. 1999. The relationship between xylem conduit diameter and cavitation caused by freeze–thaw events. *American Journal of Botany* **86**: 1367–1372.

Hacke UG, Sperry JS. 2001. Functional and ecological xylem anatomy. *Perspectives in Plant Ecology Evolution and Systematics* **4**: 97–115.

Hacke UG, Sperry JS, Ewers BE, Ellsworth DS, Schäfer KVR, Oren R. 2000a. Influence of soil porosity on water use in *Pinus taeda*. *Oecologia* **124**: 495–505.

Hacke UG, Sperry JS, Pittermann J. 2000b. Drought experience and cavitation resistance in six shrubs from the Great Basin, Utah. *Basic and Applied Ecology* **1**: 31–41.

Hacke UG, Sperry JS, Pockman WT, Davis SD, McCulloh KA. 2001. Trends in wood density and structure are linked to prevention of xylem implosion by negative pressure. *Oecologia* **126**: 457–461.

Hacke UG, Sperry JS, Wheeler JK, Castro L. 2006. Scaling of angiosperm xylem structure with safety and efficiency. *Tree Physiology* **26**: 689–701.

Holbrook NM, Burns MJ, Field CB. 1995. Negative xylem pressures in plants: a test of the balancing pressure technique. *Science* **270**: 1193–1194.

Jacobsen AL, Ewers FW, Pratt RB, Paddock WA, Davis SD. 2005. Do xylem fibers affect vessel cavitation resistance? *Plant Physiology* **139**: 546–556.

Jacobsen AL, Pratt RB. 2012. No evidence for an open vessel effect in centrifuge-based vulnerability curves of a long-vesselled liana (*Vitis vinifera*). *New Phytologist* **194**: 982–990.

Jacobsen AL, Pratt RB, Davis SD, Ewers FW. 2007. Cavitation resistance and seasonal hydraulics differ among three arid Californian plant communities. *Plant, Cell & Environment* **30**: 1599–1609.

Jacobsen AL, Pratt RB, Davis SD, Tobin MF. 2014. Geographic and seasonal variation in chaparral vulnerability to cavitation. *Madroño*, in press.

Lens F, Sperry JS, Christman MA, Choat B, Rabaey D, Jansen S. 2010. Testing hypotheses that link wood anatomy to cavitation resistance and hydraulic conductivity in the genus *Acer*. *New Phytologist* **190**: 709–723.

Li YY, Sperry JS, Taneda H, Bush SE, Hacke UG. 2008. Evaluation of centrifugal methods for measuring xylem cavitation in conifers, diffuse- and ring-porous angiosperms. *New Phytologist* **177**: 558–568.

Matzner SL, Rice KJ, Richards JH. 2001. Intra-specific variation in xylem cavitation in interior live oak (*Quercus wislizenii* A. DC.). *Journal of Experimental Botany* **52**: 783–789.

McElrone A, Brodersen C, Alsina M, Drayton W, Matthews M, Shackel K, Wada H, Zufferey V, Choat B. 2012. Centrifuge technique consistently overestimates vulnerability to water stress-induced cavitation in grapevines as confirmed with high-resolution computed tomography. *New Phytologist* **196**: 661–665.

Paddock WAS, Davis SD, Pratt RB, Jacobsen A, Tobin MF, López-Portillo J, Ewers FW. 2013. Factors determining mortality of adult chaparral shrubs in an extreme drought year in California. *Aliso* **31**: 49–57.

Pérez-Donoso AG, Greve LC, Walton JH, Shackel KA, Labavitch JM. 2007. *Xylella fastidiosa* infection and ethylene exposure result in xylem and water movement disruption in grapevine shoots. *Plant Physiology* **143**: 1024–1036.

Pittermann J, Sperry JS. 2006. Analysis of freeze-thaw embolism in conifers. The interaction between cavitation pressure and tracheid size. *Plant Physiology* **140**: 374–382.

Pittermann J, Sperry JS, Hacke UG, Wheeler JK, Sikkema EH. 2006. Inter-tracheid pitting and the hydraulic efficiency of conifer wood: the role of tracheid allometry and cavitation protection. *American Journal of Botany* **93**: 1265–1273.

Plaut JA, Yepez EA, Hill J, Pangle R, Sperry JS, Pockman WT, McDowell NG. 2012. Hydraulic limits preceding mortality in a piñon–juniper woodland under experimental drought. *Plant, Cell & Environment* **35**: 1601–1617.

Plavcova L, Hacke UG. 2011. Heterogeneous distribution of pectin epitopes and calcium in different pit types of four angiosperm species. *New Phytologist* **192**: 885–897.

Pockman WT, Sperry JS. 2000. Vulnerability to xylem cavitation and the distribution of Sonoran desert vegetation. *American Journal of Botany* **87**: 1287–1299.

Pockman WT, Sperry JS, O'Leary JW. 1995. Sustained and significant negative water pressure in xylem. *Nature* **378**: 715–716.

Pratt RB, Jacobsen AL, Ewers FW, Davis SD. 2007a. Relationships among xylem transport, biomechanics and storage in stems and roots of nine Rhamnaceae species of the California chaparral. *New Phytologist* **174**: 787–798.

Pratt RB, Jacobsen AL, Golgotiu KA, Sperry JS, Ewers FW, Davis SD. 2007b. Life history type and water stress tolerance in nine California chaparral species (Rhamnaceae). *Ecological Monographs* **77**: 239–253.

Pratt RB, Jacobsen AL, Mohla R, Ewers FW, Davis SD. 2008. Linkage between water stress tolerance and life history type in seedlings of nine chaparral species (Rhamnaceae). *Journal of Ecology* **96**: 1252–1265.

Rockwell FE, Wheeler JK, Holbrook NM. 2014. Cavitation and its discontents: opportunities for resolving current controversies. *Plant Physiology* **164**: 1649–1660.

Schreiber SG, Hacke UG, Hamann A, Thomas BR. 2011. Genetic variation of hydraulic and wood anatomical traits in hybrid poplar and trembling aspen. *New Phytologist* **190**: 150–160.

Sperry J. 2013. Cutting-edge research or cutting-edge artefact? An overdue control experiment complicates the xylem refilling story. *Plant, Cell & Environment* **36**: 1916–1918.

Sperry JS, Christman MA, Torres-Ruiz JM, Taneda H, Smith DD. 2012. Vulnerability curves by centrifugation: is there an open vessel artefact, and are 'r' shaped curves necessarily invalid? *Plant, Cell & Environment* **35**: 601–610.

Sperry JS, Donnelly JR, Tyree MT. 1988. A method for measuring hydraulic conductivity and embolism in xylem. *Plant, Cell & Environment* **11**: 35–40.

Sperry JS, Hacke UG. 2002. Desert shrub water relations with respect to soil characteristics and plant functional type. *Functional Ecology* **16**: 367–378.

Sperry JS, Hacke UG. 2004. Analysis of circular bordered pit function – I. Angiosperm vessels with homogenous pit membranes. *American Journal of Botany* **91**: 369–385.

Sun Q, Rost TL, Matthews MA. 2008. Wound-induced vascular occlusions in *Vitis vinifera* (Vitaceae): tyloses in summer and gels in winter. *American Journal of Botany* **95**: 1498–1505.

Sun Q, Sun Y, Walker MA, Labavitch JM. 2013. Vascular occlusions in grapevines with Pierce's Disease make disease symptom development worse. *Plant Physiology* **161**: 1529–1541.

Taneda H, Sperry JS. 2008. A case-study of water transport in co-occurring ring-versus diffuse-porous trees: contrasts in water-status, conducting capacity, cavitation and vessel refilling. *Tree Physiology* **28**: 1641–1651.

Tobin MF, Pratt RB, Jacobsen AL, De Guzman ME. 2013. Xylem vulnerability to cavitation can be accurately characterised in species with long vessels using a centrifuge method. *Plant Biology* **15**: 496–504.

Torres-Ruiz JM, Cochard H, Mayr S, Beikircher B, Diaz-Espejo A, Rodriguez-Dominguez CM, Badel E, Fernández JE. 2014. Vulnerability to cavitation in *Olea europaea* current-year shoots: further evidence of an open-vessel artefact associated with centrifuge and air-injection techniques. *Physiologia Plantarum*. doi: 10.1111/ppl.12185.

Torres-Ruiz JM, Sperry JS, Fernandez JE. 2012. Improving xylem hydraulic conductivity measurements by correcting the error caused by passive water uptake. *Physiologia Plantarum* **146**: 129–135.

Trifilo P, Raimondo F, Lo Gullo MA, Barbera PM, Salleo S, Nardini A. 2014. Relax and refill: xylem rehydration prior to hydraulic measurements favours embolism repair in stems and generates artificially low PLC values. *Plant, Cell & Environment*. doi: 10.1111/pce.12313.

Wang R, Zhang L, Zhang S, Cai J, Tyree MT. 2014. Water relations of *Robinia pseudoacacia* L.: do vessels cavitate and refill diurnally or are R-shaped curves invalid in *Robinia*? *Plant, Cell & Environment*. doi: 10. 1111/pce.12315.

Wheeler JK, Huggett BA, Tofte AN, Rockwell FE, Holbrook NM. 2013. Cutting xylem under tension or supersaturated with gas can generate PLC and the appearance of rapid recovery from embolism. *Plant, Cell & Environment* **36**: 1938–1949.